Mechanisms of Maurotoxin Action on Shaker Potassium Channels

Vladimir Avdonin,* Brian Nolan,* Jean-Marc Sabatier,† Michel De Waard,‡ and Toshinori Hoshi*

*Department of Physiology and Biophysics, The University of Iowa, Iowa City, Iowa 52242 USA; and ‡Laboratoire de Neurobiologie des Canaux Ioniques and †Laboratoire de Biochimie, UMR 6560, Faculté de Médecine Nord, Institut Fédératif Jean Roche, Institut National de la Santé et de la Recherche Médicale U464, 13916 Marseille Cedex 20, France

ABSTRACT Maurotoxin (α-KTx6.2) is a toxin derived from the Tunisian chactoid scorpion *Scorpio maurus palmatus*, and it is a member of a new family of toxins that contain four disulfide bridges (Selisko et al., 1998, *Eur. J. Biochem.* 254:468–479). We investigated the mechanism of the maurotoxin action on voltage-gated K^+ channels expressed in *Xenopus* oocytes. Maurotoxin blocks the channels in a voltage-dependent manner, with its efficacy increasing with greater hyperpolarization. We show that an amino acid residue in the external mouth of the channel pore segment that is known to be involved in the actions of other peptide toxins is also involved in maurotoxin's interaction with the channel. We conclude that, despite the unusual disulfide bridge pattern, the mechanism of the maurotoxin action is similar to those of other K^+ channel toxins with only three disulfide bridges.

INTRODUCTION

Scorpion toxins constitute the largest group of potassium channel toxins. They are generally small peptides 29–39 amino acids in size with a net positive surface charge under physiological conditions. Many of these toxins exhibit a very similar three-dimensional folding motif that contains a short α-helix and an antiparallel β-sheet of two or three strands, depending on the length of the amino terminus (Miller, 1995). Recently, structures of unusual toxins containing an additional disulfide bridge were reported, which include Pi1 isolated from *Pandinus imperator* (Olamendi-Portugal et al., 1996), maurotoxin from *Scorpio maurus* (Kharrat et al., 1997), and HsTX1 from *Heterometrus spinnifer* (Lebrun et al., 1997). Maurotoxin (α-KTx6.2), for instance, is a short peptide toxin comprising 34 amino acid residues isolated from the Tunisian chactoid scorpion (Kharrat et al., 1997; Rochat et al., 1998). This toxin represents ~0.6% of the total protein in the total crude venom, and the presence of four disulfide bridges was confirmed by an NMR analysis (Kharrat et al., 1996). Previously, the presence of four disulfide bridges was considered a hallmark characteristic of the toxins that block voltage-gated Na^+ channels (Catterall and Beneski, 1980). In contrast, those toxins that affect voltage-gated K^+ channels, such as charybdotoxin (CTX), contain three disulfide bridges (Miller, 1995). However, physiological studies indicate that maurotoxin, with four disulfide bridges, may block selected voltage-dependent K^+ channels (Rochat et al., 1998).

Mechanisms of the actions of the three-disulfide bridge K^+ channel toxins have been studied extensively (MacKinnon and Miller, 1988; Goldstein and Miller, 1993). These toxins often act to plug the K^+ channel ion conduction pore (MacKinnon and Miller, 1988). The toxin association rate constants are voltage-independent, whereas the dissociation rate constants are frequently voltage-dependent, typically sensing up to 35% of the membrane electric field (Hermann and Erxleben, 1987). Because maurotoxin contains four disulfide bridges (Kharrat et al., 1996), it may be hypothesized that the mechanism of the toxin action on voltage-dependent K^+ channels may be different from those of the three disulfide bridge toxins, such as CTX. To better investigate the biophysical and molecular mechanisms of the maurotoxin action on voltage-gated K^+ channels with less confounding variables, we used mutant Shaker channels without fast inactivation (Hoshi et al., 1990) expressed in *Xenopus* oocytes. The macroscopic and single-channel results show that the toxin's efficacy is dependent on the membrane voltage and K^+ ions, and that an amino acid residue in the external mouth of the channel pore contributes to its action. Despite the difference in the disulfide bond pattern, the blocking mechanism of maurotoxin appears to be similar to those of other K^+ channel peptide toxins.

MATERIALS AND METHODS

Channel expression

Shaker K^+ channels were expressed in *Xenopus* oocytes by RNA injection essentially as described (Hoshi et al., 1990). ShBΔ6–46 contains a 41-residue deletion in the amino terminus and lacks N-type inactivation (Hoshi et al., 1990). ShBΔ6–46:T449V and ShBΔ6–46:T449Y contain a single amino acid substitution at position 449 (using the ShB numbering) from T to V and from T to Y, respectively (López-Barneo et al., 1993). These channels show very slow P/C-type inactivation when expressed in oocytes (Hoshi et al., 1991). The RNAs were transcribed using T7 RNA polymerase (Ambion, Austin, TX) and injected into the oocytes (45 nl/cell). Recordings were typically made 1–14 days after injection.

Electrophysiological recording

Two-electrode voltage clamp (TEV) recordings were made using a Warner OC-725B amplifier (Warner, Hamden, CT). The electrodes filled with 3 M

Received for publication 22 December 1999 and in final form 24 April 2000.

Address reprint requests to Dr. Toshinori Hoshi, Department of Physiology and Biophysics, Bowen 5660, The University of Iowa, Iowa City, IA 52242. Tel.: 319-335-7845; Fax: 319-353-5541; E-mail: hoshi@hoshi.org.

0006-3495/00/08/776/12 $2.00

KCl had a typical initial resistance of less than 0.8 MΩ. The vitelline membrane of the oocyte was left intact. The macroscopic patch and single-channel recordings were performed as described (Hamill et al., 1981; Methfessel et al., 1986). The macroscopic patch currents were low-pass filtered through an eight-pole Bessel filter unit with a corner frequency of 2 kHz and digitized at 10 kHz, using an ITC16 interface (Instrutech, Port Washington, NY). The data were collected and analyzed using Patch Machine (http://www.hoshi.org), Pulse (Heka, Lambrecht, Germany), and Igor Pro (Wavemetrics, Lake Oswego, OR) running on Apple Macintosh computers. Unless otherwise indicated, linear capacitative and leak currents have been subtracted from the macroscopic currents presented, using a modified *P/n* protocol as implemented in Pulse and Patch Machine. The single-channel data were filtered at 5 kHz and digitized at 25 kHz. The Hidden Markov model (Chung and Gage, 1998) was used to idealize the single-channel records as implemented in Patch Machine. When appropriate, the data values are presented as means ± SD. The error bars are not shown when they are smaller than the symbol size. All experiments were performed at room temperature (20–24°C).

Solutions

The intracellular solution typically contained (in mM) 140 KCl, 2 $MgCl_2$, 11 EGTA, 10 HEPES (pH 7.2) (*N*-methyl glucamine). The standard extracellular solution contained (in mM) 140 NaCl, 2 $MgCl_2$, 2 KCl, 10 HEPES (pH 7.2) (*N*-methyl glucamine). Other solutions used are indicated in the legends. The toxin was chemically synthesized by the optimized solid-phase technique described previously (Kharrat et al., 1996). The stock toxin solution (30 μM) was prepared and added to the physiological recording solutions as required to achieve the desired concentrations. Unused portions of the solutions were kept frozen at −20°C.

RESULTS

The ShBΔ6–46 channel has a large deletion in the N terminus to effectively abolish fast N-type inactivation mediated by the ball-and-chain mechanism (Hoshi et al., 1990). C-type inactivation is retained in this channel, but the inactivation time course in the presence of a few mM of external K^+ is much slower than the channel activation time course (Hoshi et al., 1991). Fig. 1 *A* illustrates the effects of different concentrations of maurotoxin applied to the extracellular solution on the ShBΔ6–46 currents recorded at +50 mV, using two-electrode voltage clamp in the presence of 2 mM external [K^+]. With increasing concentrations of the toxin, from 3 nM to 1 μM, the peak current amplitude became progressively smaller. The blocking effects were readily reversed by washing the recording chamber. With higher toxin concentrations, an additional slower rising phase in the current time course became much more prominent, such that the control current and the currents recorded in the presence of high concentrations of the toxin did not follow the same overall time course.

The toxin's effect of modifying the current time course is further illustrated in Fig. 1 *B*. The graph shows the amount of block by the toxin as a function of time during the depolarization epoch, with unity representing the complete block or no current in the presence of the toxin. If the blocking effect is independent of time during depolarization, straight horizontal lines should result. However, the results show that the block became less effective with time during depolarization. Other peptide K^+ channel blockers with three disulfide bonds are also known to induce a slow rising phase in the current time course on depolarization similar to that observed here (Fig. 1 *A*), and it has been interpreted to indicate toxin dissociation from the channel during depolarization (Garcia et al., 1999; Terlau et al., 1999). Thus our working model is that the slow phase during depolarization in the presence of the toxin represents the unblock time course; the toxin becomes less effective with depolarization. According to this model, the initial (t = 0) value indicates the fraction of the channels that were blocked by the toxin immediately before the pulse onset at the holding voltage (−90 mV), and the steady-state value reflects the fractional block at the new test voltage (+50 mV in Fig. 1 *A*). At every concentration examined, the toxin was more effective at the holding voltage, and it became less effective when depolarized to +50 mV, thus slowly increasing the current amplitude.

We found that the unblock time course (Fig. 1 *B*) was adequately described by a single exponential, suggesting that the following simple model may be sufficient to account for the unblock phenomenon observed in the voltage range of −20 to +50 mV:

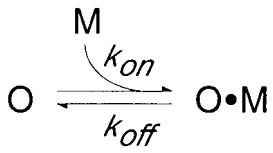

Scheme A

where O·M represents the toxin (M)-blocked nonconducting state and O represents the unblocked open state. According to this model, depolarization shifts the equilibrium toward the open state (O) by decreasing k_{on} and/or increasing k_{off}, thus enhancing the current amplitude with time, as shown in Fig. 1 *A*.

Because the efficacies of the toxin in reducing the current amplitude were different at different times during depolarization, we measured the concentration dependence by fitting the unblock time course with a single exponential. The extrapolated initial (t = 0) values and the steady-state values were used separately to obtain the toxin concentration dependence (Fig. 1 *C*). The toxin is more effective in reducing the current amplitude at the beginning of the pulse (Fig. 1 *C*, *empty circles*) than later in the pulse (Fig. 1 *C*, *filled circles*), shifting the IC_{50} value by a factor of 10 from 130 to 10 nM (Fig. 1 *C*). Within the framework of our working model, the concentration dependence based on the measurements at beginning of the pulse reflects the channel's sensitivity to the toxin at the holding voltage (−90 mV), and the steady-state measurements represent the channel's sensitivity at a test voltage of +50 mV. The toxin is clearly more effective at the holding voltage. The concen-

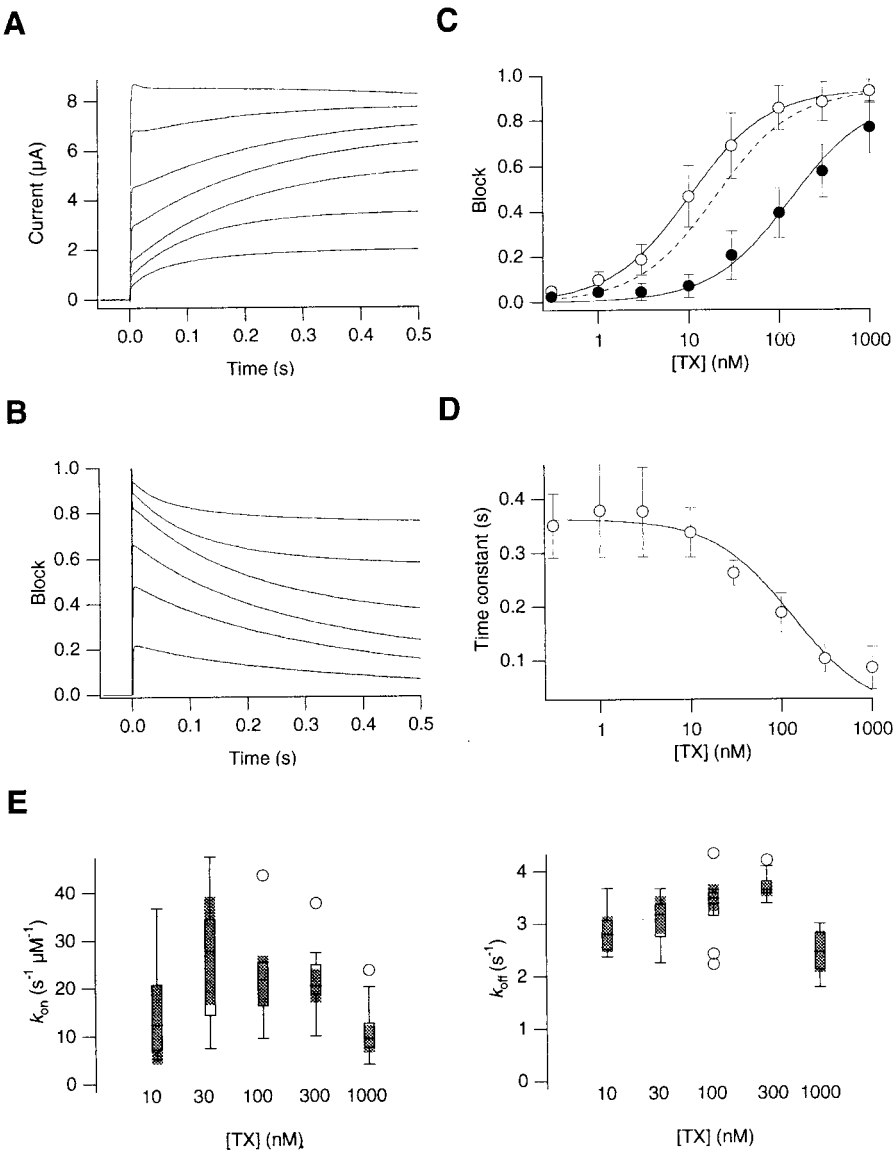

FIGURE 1 Maurotoxin block of ShBΔ6–46 currents. (*A*) Representative ShBΔ6–46 currents at +50 mV recorded using two-electrode voltage clamp in the presence of different concentrations of maurotoxin (0, 3, 10, 30, 100, 300 and 1000 nM, *from top to bottom*). The extracellular solution contained 2 mM KCl. The currents were elicited by pulses from −90 mV to +50 mV. (*B*) Time-dependent unblocking of the channel currents at +50 mV for the current sweeps shown in *A*. The difference between the currents with and without the toxin was divided by the control current at every time point. The toxin block decreases with time, following a single exponential time course. (*C*) Concentration dependence of the toxin block. The block time course shown as calculated in *B* was fitted with a single exponential. The extrapolated $t = 0$ values (○) and the steady-state block values are plotted against the toxin concentration. Smooth curves are Langmuir isotherms. Block $= f \cdot [TX]/([TX] + K^{DISS})$, where K^{DISS} is a dissociation constant, and f is a scaling factor to account for a small fraction of the channels inaccessible to toxin in the TEV recording. The solid curves represent the best fits. The dashed curve shows the concentration dependence of the initial block ($t = 0$) estimated from extrapolation of the rate constants obtained at depolarized voltages in response to pulses from −90 mV (see text). (*D*) Concentration dependence of the time constant of unblocking. The block time course (see *B*) was fitted with a simple exponential, and the time constant values, estimated with different toxin concentrations, are plotted. The smooth line represents the best fit with $1/(k_{off} + k_{on}\cdot[TX])$, with the ratio $K^{DISS} = k_{off}/k_{on}$ determined from the concentration dependence of the steady-state block as shown in *C*. (*E*) Rate constants of the unblock time course at +50 mV in the presence of different concentrations of the toxin. The rate constants were computed from the fractional block measurements (Block) and the time constants of current relaxation (τ) as follows: $k_{on} = \text{Block}/([TX]\cdot\tau)$, $k_{off} = (1 - \text{Block})/\tau$.

tration dependence results shown in Fig. 1 *C* were fit well by simple Langmuir isotherms (*smooth solid curves*; see Fig. 1 *C* legend), further supporting the simple model above as adequate to describe the toxin blocking/unblocking action. This observation, in turn, is consistent with the idea that one toxin molecule is sufficient to block the channel.

The concentration dependence of the unblock time course was analyzed by fitting the data with an exponential, and the time constant values are plotted in Fig. 1 *D*. From the unblock time course and the fractional block measurements, it is possible to estimate the k_{on} and k_{off} values in Scheme A. As predicted by the model, both k_{on} and k_{off} were independent of the toxin concentration, being $\sim 18 \pm 6\ s^{-1} \cdot \mu M^{-1}$ and $3.3 \pm 0.8\ s^{-1}$ at +50 mV, respectively (Fig. 1 *E*).

The unblock time course became more prominent with greater depolarization. The ShBΔ6–46 currents recorded at different voltages, from −60 to +50 mV, in the presence of the toxin (300 nM) are shown in Fig. 2 *A*. At the voltages more positive than −20 mV, the open channel probability is nearly saturated at 0.85–0.9 (Hoshi et al., 1994; also see Fig. 3 *A*). With greater depolarization, the unblock time course was very obvious, clearly indicating that the toxin block became much less effective with greater depolarization. For example, at +50 mV, the current amplitude at the end of the 500-ms pulse was roughly three times greater than the initial current amplitude. The time course of unblocking at different voltages is illustrated in Fig. 2 *B*.

The voltage dependence of the unblocking time course was further analyzed with the simple two-state model described above. From the time constant values and the steady-state fractions of the channels blocked, we obtained the effective blocking and unblocking rate constant values (k_{on} and k_{off}; see scheme A); their voltage dependence is shown in Fig. 2 *C*. In the voltage range of −20 to +50 mV, where the channel open probability is nearly saturated, the block rate constant, k_{on}, did not show much voltage dependence, whereas the unblock rate constant, k_{off}, showed marked voltage dependence with an effective valence of 0.37 ± 0.09. This equivalent charge indicates that k_{off} decreases by *e*-fold with every 70 mV of hyperpolarization. Assuming that the same voltage dependence extends to more negative voltages, the extrapolated k_{off} value at the holding voltage of −90 mV is $0.4\ s^{-1}$, while at +50 mV, the measured k_{off} value was $3.3\ s^{-1}$. Thus this voltage dependence of k_{off} is likely to contribute to the voltage-dependent unblocking time course observed with depolarization to the range of −30 to +50 mV. If it is further assumed that k_{on} is voltage independent down to −90 mV, it is possible to estimate the concentration dependence as shown in Fig. 1 *C* (*dashed line*). The estimated concentration dependence with $IC_{50} = 20$ nM is similar to but not identical with the concentration dependence obtained from the measurements at the beginning of the pulse (*open circles*; $IC_{50} = 10$ nM), which should reflect the fraction of the channels that are blocked at the holding voltage before the pulse onset.

We investigated the toxin action at the single-channel level and observed that the channel opening time course was often slower in the presence of the toxin. Representative records illustrating this characteristic are shown in Fig. 3 *A*. As shown previously (Hoshi et al., 1994), in response to step depolarization, the ShBΔ6–46 channel opened fast and

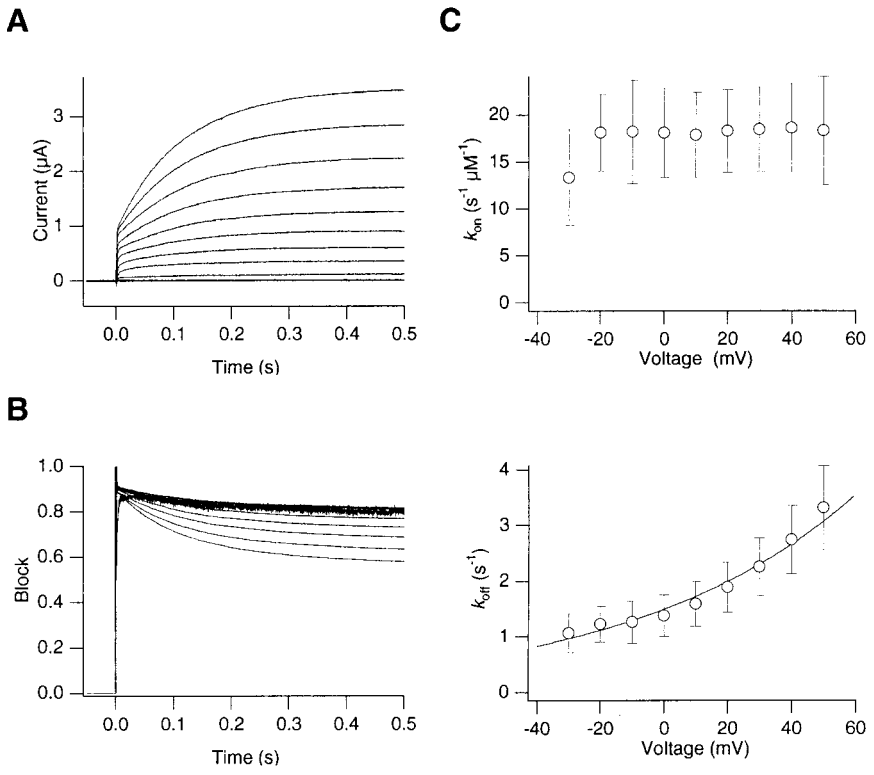

FIGURE 2 Voltage dependence of the toxin block. (*A*) Representative ShBΔ6–46 currents at different voltages recorded in the presence of maurotoxin (300 nM). The currents were elicited by pulses from −60 mV to +50 mV in 10-mV increments. (*B*) Unblocking time course at different voltages. The fractional block time course for the sweeps in *A* was calculated as in Fig. 1 *B*. (*C*) The toxin block and unblock rate constants at different voltages (see Scheme A). Because the rate constant values are independent of the toxin concentration, the results from three toxin concentrations (30, 100, and 300 nM) were pooled. The smooth line represents an exponential fit to the data.

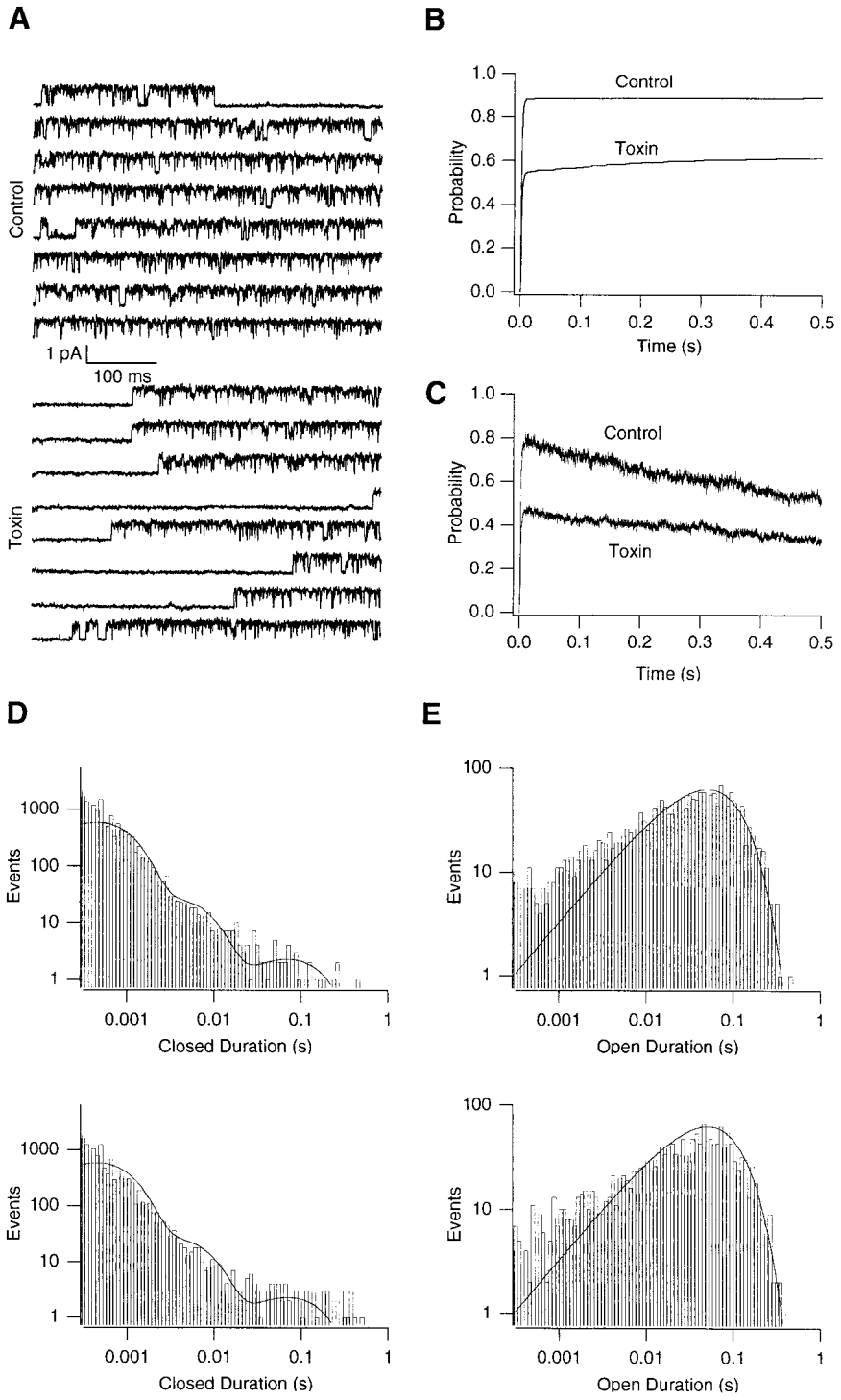

FIGURE 3 Block of single ShBΔ6–46 channel currents by maurotoxin. (*A*) Single-channel records in response to pulses from −90 to 0 mV before (*upper panel*) and after (*lower panel*) application of the toxin (5 nM). Those current traces that illustrate the effect of the toxin of delaying the opening process were selected and displayed. Only the traces with significant delay before the first opening after toxin application are shown. (*B*) First latency distributions on the single-channel events before and after toxin application (5 nM). The distributions contained 300 and 400 events in the control and toxin groups, respectively. (*C*) Ensemble averages for the experiment shown in *A*. (*D*) Closed duration histograms before (*upper panel*) and after (*lower panel*) application of 5 nM maurotoxin. The smooth curves on the two panels are the same and represent the best fit to the control histogram with three exponential components (time constants 0.5, 3.4, and 70 ms). (*E*) Open duration histograms before (*upper panel*) and after (*lower panel*) application of 5 nM maurotoxin. The smooth curves on the two panels are the same and represent the best single exponential fit to the control histogram (time constants 50 ms). The results presented in this figure come from the same single-channel patch.

stayed open continually in most of the recording epochs. In the presence of the toxin, however, the channel sometimes opened more slowly, often requiring a few hundred milliseconds before the first opening. The first latency distributions recorded before and after toxin application are compared in Fig. 3 *B*. In the control condition, ~90% of the depolarizing pulses elicited at least one opening, and almost all of the first openings were observed within 9 ms of the depolarization onset. In the presence of the toxin, however, there were significantly more apparent null sweeps where the channel failed to open in response to depolarization, and a slower "creep up" phase in the first latency distribution

was also observed. In the results shown in Fig. 3 *B*, the toxin increased the fraction of "null" sweeps from 10% to 40%. This observation is consistent with the macroscopic analysis presented in Fig. 1, which suggests that k_{off} at hyperpolarized voltages is very small. According to the working model presented earlier, the null sweeps represent those depolarization epochs that failed to remove the toxin from the channel and the toxin remained bound to the channel. The time course of the slow first latency events from single-channel patches was fitted with an exponential. The rate constants estimated from the fits (1.3, 1.5, and 4.4 s^{-1}) were similar to the k_{off} value (1.4 ± 0.4 s^{-1}) obtained from the macroscopic current measurements (see Fig. 2 *B*). The slow first latency events, therefore, likely represent the unblock time course. The two first latency distributions in Fig. 3 *B*, whether the null sweeps were considered or not, were statistically different (Kolmogrov-Smirnov test, $p = 6 \times 10^{-18}$ and 0.001 with and without null sweeps, respectively). Consistent with the increased fraction of null sweeps, the ensemble averages showed that the toxin indeed decreased the peak open probability (Fig. 3 *C*). Similar results were obtained from two other single-channel patches.

The toxin markedly increased the null fraction and slowed the first latency distribution; however, it did not affect the gating behavior of the channel once it opened. The open and closed durations measured before and after toxin application (5 nM) are shown in Fig. 3, *D* and *E*, respectively. These duration data were essentially unchanged by the toxin. Similar data were obtained from two other single-channel patches. The single-channel amplitudes at 0 and +50 mV were not affected by the toxin (data not shown). These single-channel results suggest that the toxin's main actions are to reduce the number of channels available to open and to lengthen the first latency.

Maurotoxin (5 nM) increased the null fraction from 0.1 to 0.4 (Fig. 3 *B*). This would effectively induce a 30% decrease in the number of channels available to open. Our macroscopic current data in Fig. 1 show that 5 nM maurotoxin decreases the initial macroscopic current by 25–30%. Thus the single-channel and macroscopic current results are in agreement with each other. The increase in the null sweeps caused by maurotoxin largely determines the decrease in the peak macroscopic current amplitude.

Blocking effects of some peptide toxins on K^+ channels are known to be dependent on external $[K^+]$. For example, the effects of CTX and κ-conotoxin PVIIA are diminished by greater external $[K^+]$ (Miller, 1995; Terlau et al., 1999; Anderson et al., 1988). K^+ channels are thought to contain multiple K^+ binding sites, and the occupancy of K^+ in the outermost binding site is considered to accelerate the toxin dissociation rate (MacKinnon and Miller, 1988). We examined whether the action of maurotoxin was also dependent on external $[K^+]$. Representative ShBΔ6–46 currents recorded in the presence of the toxin (100 nM), with different external K^+ concentrations ranging from 2 to 140 mM, are shown in Fig. 4 *A*. With different external $[K^+]$, the steady-state fractions blocked at +50 mV were similar, ~50%. However, the blocked fractions at the beginning of the pulse, representing the toxin efficacy at the holding voltage of −90 mV before the pulse onset, were markedly different (Fig. 4, *A* and *B*). With 2 mM external $[K^+]$, the initial current amplitude was near zero, suggesting that nearly all of the channels were blocked before the pulse onset and were unavailable to open. With 100 mM $[K^+]$, the initial current amplitude was much greater, ~40% of the control value. This indicates that ~40% of the channels were unblocked and available to open before the pulse onset. The fractional number of channels available to open ranged from near 0 to 40% when the external $[K^+]$ was changed from 2 to 100 mM (Fig. 4 *B*).

We examined how the external $[K^+]$ and voltage interacted to influence the toxin efficacy. The concentration dependence of the toxin block at the pulse onset (*open symbols*), representing the toxin efficacy at the holding voltage of −90 mV, and that at the end of the depolarization pulse at +50 mV (*closed symbols*) in the presence of 2 mM (*squares*) and 100 mM (*circles*) external $[K^+]$, are compared in Fig. 4 *C*. With 2 mM $[K^+]$, the channel at −90 mV (IC_{50} = 10 nM) is almost an order of magnitude more sensitive to the toxin than at +50 mV (IC_{50} = 80 nM, compare the *open* and *closed squares* in Fig. 4 *C*). However, with 100 mM $[K^+]$, this voltage dependence was significantly less than that with 2 mM $[K^+]$, and the concentration dependence curves obtained from the beginning and the end of the pulse were similar (*circles* in Fig. 4 *C*).

The voltage dependence of k_{on} and k_{off} in the presence of 100 mM $[K^+]$ is shown in Fig. 4 *D*. As found in the presence of 2 mM $[K^+]$, k_{on} was essentially voltage independent in the range examined. The dissociation rate constant k_{off} was voltage dependent, decreasing with hyperpolarization with an equivalent charge of 0.7 ± 0.1. The estimated equivalent charge, however, was greater than that found with 2 mM $[K^+]$ (0.37; see Fig. 2). If the voltage dependence of k_{off} extends down to −90 mV, the k_{off} value at −90 mV is extrapolated to be 0.06 s^{-1}, which is noticeably smaller than that found with 2 mM $[K^+]$ (0.4 s^{-1}). If we further assume that k_{on} is voltage independent, these rate constant values predict the IC_{50} value of 3 nM at −90 mV in the presence of 100 mM $[K^+]$. This predicted value is much lower than the observed value of 80 nM (see the *filled squares* in Fig. 4 *C*). With 2 mM $[K^+]$, the voltage dependence of k_{off} roughly but not totally accounts for the toxin action needed to decrease the number of channels available to open at −90 mV (Fig. 1). With high $[K^+]$, however, the actual k_{off} values at negative voltages must be appreciably greater than the extrapolated values obtained from the unblock time course at more positive voltages.

Some blockers of ion channels are known to be "knocked off" by ion fluxes through the channel pores (Park and Miller, 1992). For example, charybdotoxin bound to high-

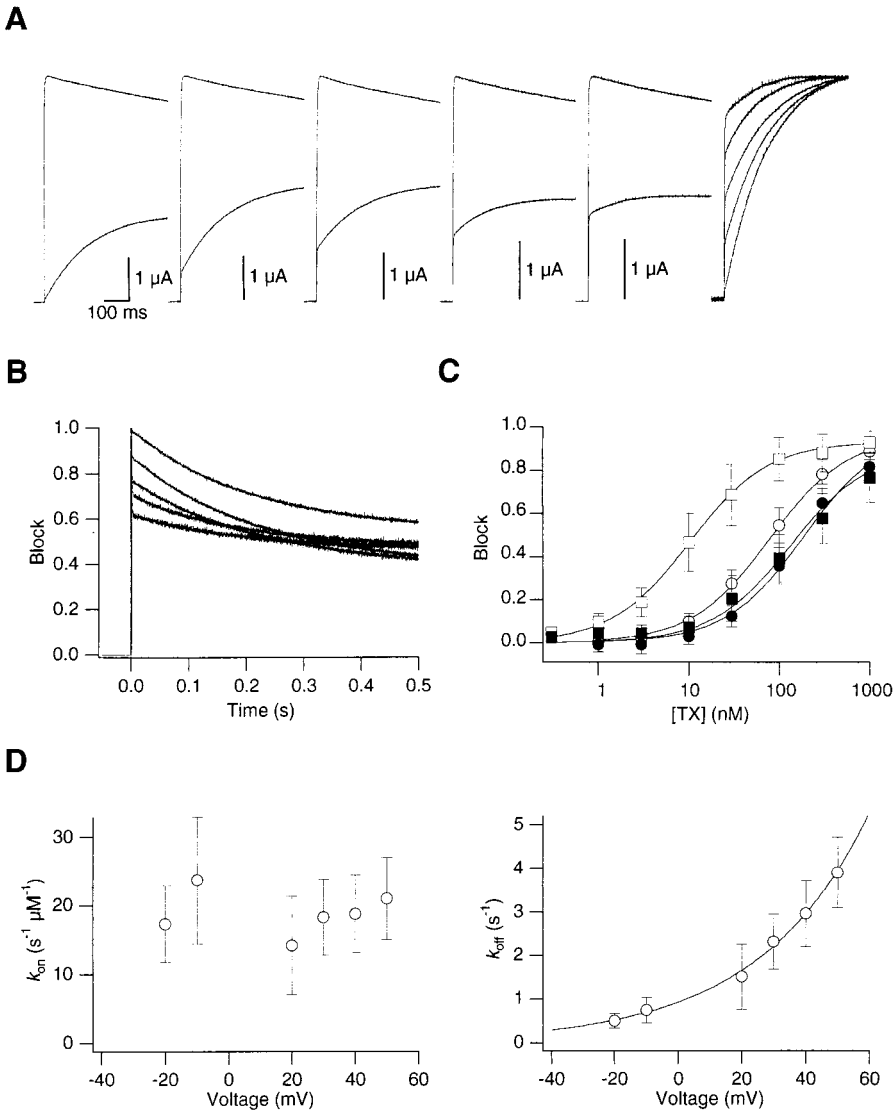

FIGURE 4 Effect of external $[K^+]$ on the maurotoxin block. (*A*) Representative currents recorded using TEV at +50 mV in the presence of different external $[K^+]$ with and without 100 nM maurotoxin. External $[K^+]$ was 2, 10, 30, 100, and 140 mM (*from left to right*). At each external $[K^+]$ examined, the control current was obtained and then the toxin (100 nM) was added to the bath. The rightmost panel shows the scaled currents recorded in the presence of the toxin to illustrate the unblocking time course. (*B*) The unblocking time course with different external $[K^+]$. The fractional block values at each time point were calculated as in Fig. 1 *B*. (*C*) Concentration dependence of the block with 2 mM and 100 mM external $[K^+]$. For each external $[K^+]$, the concentration dependence was measured from the initial current ($t = 0$) values and from the steady-state current values at +50 mV as in Fig. 1 *C*. □, $t = 0$, 2 mM $[K^+]$; ○, $t = 0$, 100 mM $[K^+]$; ■, steady state, 2 mM $[K^+]$; ●, steady state, 100 mM $[K^+]$. (*D*) Voltage dependence of the toxin block rate constants with 100 mM external $[K^+]$. The solid line in the right panel shows an exponential fit with an equivalent charge of 0.73 *e*.

conductance Ca^{2+}-activated K^+ channels can be destabilized by K^+ entering the channel from the opposite, internal solution. This property is mediated by K27 on charybdotoxin (Miller, 1995), which is equivalent to K23 in maurotoxin. Thus we attempted to determine whether maurotoxin could be knocked off by an efflux of K^+ through the channel pore. We kept the external $[K^+]$ constant at 100 mM to minimize the fractional changes in the external $[K^+]$ concentration and varied the internal $[K^+]$. If the toxin is knocked off by K^+ efflux, the unblock time course should be slow with lower internal $[K^+]$ and faster with high internal $[K^+]$. Scaled representative currents recorded in the presence of maurotoxin (100 nM) with three different internal $[K^+]$ are shown in Fig. 5 *A*. With 20 mM internal $[K^+]$, the unblock time course was very slow and was barely observed. With higher internal $[K^+]$, the unblock time course became more noticeable and faster. These results indicate that efflux of K^+ does influence the toxin efficacy, consistent with the idea that K^+ efflux knocks off the toxin. Thus the "knock-off" phenomenon is likely to contribute to the voltage dependence of k_{off} in the voltage range in which the channels are open.

The results obtained with different concentrations of external $[K^+]$ indicate that the toxin action is regulated by K^+. C-type inactivation of the Shaker channel is dependent on external $[K^+]$, and the K^+ occupancy in the external mouth of the pore interferes with C-type inactivation (López-Barneo et al., 1993). In the absence of K^+ on both sides of the membrane, the C-type inactivated state allows measurable Na^+ flux (Starkus et al., 1997). We tested whether the toxin blocks the Na^+ current through the C-type inactivated state. Fig. 5 *B* shows the ionic currents recorded in the absence of both internal and external K^+ ions. In response to step depolarization to +50 mV, a transient outward Na^+

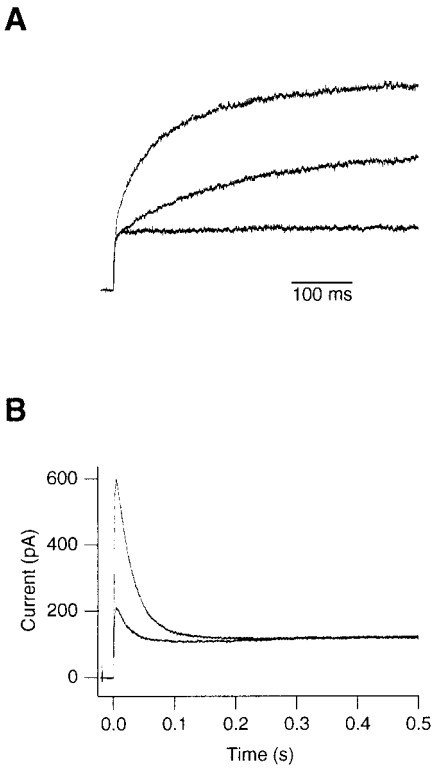

FIGURE 5 (*A*) Representative ShBΔ6–46 currents recorded in the inside-out configuration with different internal [K^+] concentrations. The current traces are scaled so that the initial unblocked amplitudes are about the same. The external solution contained 30 nM maurotoxin and 100 mM [K^+]. Internal [K^+] was 20, 100, and 300 mM (*from bottom to top*). The currents were elicited by pulses from −90 to +50 mV. (*B*) Maurotoxin block (30 nM) of ShBΔ6–46 channels in the absence of external and internal [K^+]. The currents were recorded in response to pulses from −90 to +50 mV in the absence of added [K^+], using the outside-out patch-clamp configuration. NaCl replaced KCl in the recording solutions.

current is observed, representing the fast C-type inactivation time course (Starkus et al., 1997). In addition, an appreciable amount of steady-state current was also observed, which is considered to reflect Na^+ efflux through the C-type inactivated state (Starkus et al., 1997). Maurotoxin (30 nM) decreased the amplitude of the transient current, representing Na^+ flux through the open state. However, the toxin did not affect the steady-state component mediated by Na^+ through the C-type inactivated state. The results suggest that the toxin may preferentially interact with the open state of the channel but not with the C-type inactivated state.

We investigated which amino acid residues of the channel protein are involved in the toxin efficacy. We hypothesized that position 449 in the external mouth of the ShB channel is important for the toxin action for the following reasons. First, effects of other K^+ channel blockers, such as CTX and tetraethyl ammonium (TEA), are known to be mediated partly by the 449 residue (Naranjo and Miller, 1996; Molina et al., 1997). Second, the channel's sensitivity to the toxin is dependent on external [K^+], and the 449 position influences C-type inactivation, which is also dependent on external [K^+] (López-Barneo et al., 1993). Thus we compared the effects of the toxin on ShBΔ6–46:T449T (wild type), ShBΔ6–46:T449V, and ShBΔ6–46:T449Y. The ShBΔ6–46:T449Y and T449V channels were selected because these mutants normally show very slow C-type inactivation (López-Barneo et al., 1993), thus avoiding confounding with fast C-type inactivation when the results are compared with those from the wild-type channels (ShBΔ6–46). Representative ShBΔ6–46:T449Y (panel *A*) and ShBΔ6–46:T449V (panel *B*) currents recorded with two-electrode voltage-clamp at 0 mV in the presence of maurotoxin and of TEA are shown in Fig. 6. With Y at position 449, the channel is not noticeably affected by maurotoxin but is very efficiently blocked by external TEA. With V at position 449, the channel was well blocked by maurotoxin but very resistant to external TEA. The concentration dependence obtained for the ShBΔ6–46:T449T, ShBΔ6–46:T449Y, and ShBΔ6–46:T449V channels is shown in Fig. 6 *C*. The ShBΔ6–46:T449Y channel was not affected by even 100 nM maurotoxin (Fig. 6 *C*). Thus the toxin efficacy of the ShBΔ6–46 channel is influenced by the amino acid at position 449 in the external mouth of the channel.

C-type inactivation in ShBΔ6–46:T449V and ShBΔ6–46:T449Y expressed in oocytes is very slow, and its time course is little affected by external [K^+]. We investigated how maurotoxin affected the ShBΔ6–46:T449V channel in the presence of low and high external [K^+]. The fractional blocks were measured from exponential fits as in Fig. 1; the results are shown in Fig. 6 *E*. With the ShBΔ6–46 channel, which shows noticeable C-type inactivation depending on external [K^+] (López-Barneo et al., 1993), the concentration dependence at negative voltages was markedly different for the low and high external [K^+] conditions (*squares* versus *circles* in Fig. 4 *C*). With the ShBΔ6–46:T449V channel, the two concentration dependence curves were markedly closer to each other, and the IC_{50} values were 22 and 54 nM (*open squares* versus *open circles* in Fig. 6 *E*). Thus, compared with the ShBΔ6–46 channel, the toxin block of the ShBΔ6–46:T449V channel is less dependent on external [K^+].

DISCUSSION

We showed here that maurotoxin reduces ionic currents through Shaker K^+ channels by decreasing the probability that the channel enters the nonblocked open state in response to depolarization. Furthermore, our results show that the toxin preferentially blocks the channels at hyperpolarized voltages and that the blocking efficacy is regulated by both external and internal [K^+]. The amino acid residue at position 449 in the external mouth of the pore contributes to the channel's sensitivity to the toxin. The macroscopic current time course in the presence of the toxin is in general

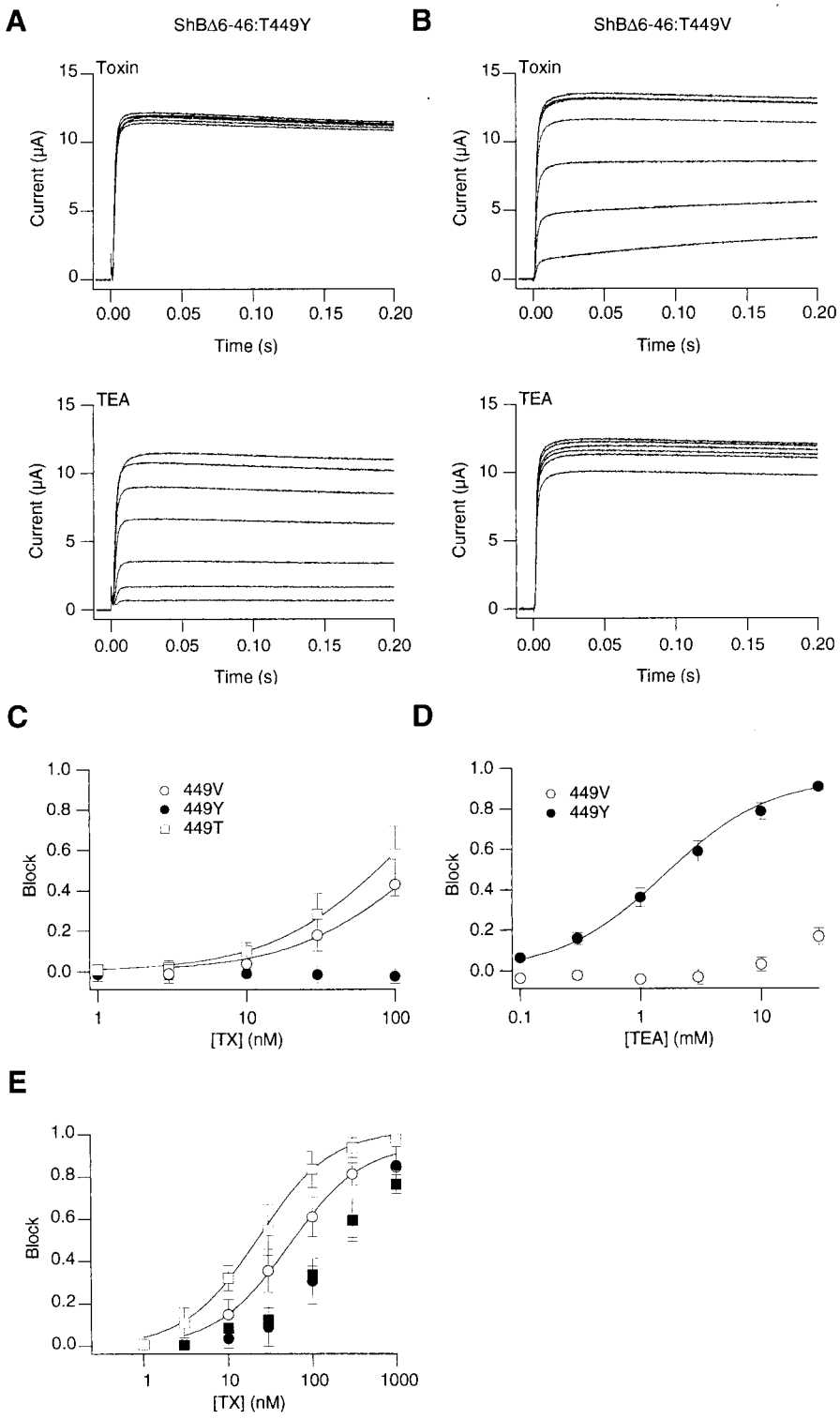

FIGURE 6 Residue 449 is important for the maurotoxin action. (*A*) Representative currents recorded using TEV from ShBΔ6–46:T449Y channels in the presence of maurotoxin (*upper panel*; 0, 3, 1, 10, 30, and 100 nM) and TEA (*lower panel*; 0.1, 0.3, 1, 10, and 30 mM). The toxin and TEA were applied to the extracellular medium. (*B*) Representative currents recorded using TEV from ShBΔ6–46:T449V channels in the presence of maurotoxin (*upper panel*; 0, 3, 1, 10, 30, and 100 nM) and TEA (*lower panel*; 0.1, 0.3, 1, 10, and 30 mM). (*C*) Steady-state concentration dependence of the maurotoxin block of ShBΔ6–46:T449T (□), ShBΔ6–46:T449Y (●), and ShBΔ6–46:T449V (○). (*D*) Concentration dependence of external TEA block of ShBΔ6–46:T449Y (●) and ShBΔ6–46:T449V (○). All data in *A–D* were recorded using pulses from −90 to 0 mV. The external solution contained 10 mM $[K^+]$. (*E*) Effect of external $[K^+]$ on the maurotoxin block of ShBΔ6–46:T449V and ShBΔ6-46: T449V currents. The extrapolated initial ($t = 0$) and steady-state values are plotted against the toxin concentration. □, $t = 0$, 2 mM $[K^+]$; ○, $t = 0$, 140 mM $[K^+]$; ■, steady state, 2 mM $[K^+]$; ●, steady state, 140 mM $[K^+]$. Note that the difference between the results from 2 and 140 mM $[K^+]$ at $t = 0$ (□ versus ○) is smaller than that found for the ShBΔ6–46:T449T channel (see Fig. 4 *C*).

consistent with the simple bimolecular scheme presented earlier (Scheme A).

The Shaker channel has several electrophysiologically distinguishable conformational states. Our results suggest that maurotoxin interacts preferentially with the closed state of the channel. This conclusion is based in part on the observations that the macroscopic current slowly increases during depolarization and that the first latency is slowed in the presence of maurotoxin, leading to the unblock phenomenon. The Na^+ conduction through the C-type inactivated

state (Starkus et al., 1997) appears to be little affected by the toxin.

The analysis of the unblock time course suggests that the block (ON) rate constant is voltage independent, while the unblock (OFF) rate constant decreases with hyperpolarization with an equivalent charge of 0.37. In the presence of low external [K^+], extrapolation of the voltage dependence of k_{off} to more negative voltages approximates the IC_{50} value based on the measurements at the beginning of the pulse, which should reflect the channel sensitivity to the toxin at the holding voltage (Fig. 1 *C*). Thus, at least with low external [K^+], the voltage dependence of k_{off} obtained from the unblock time course roughly determines whether the channel opens in response to depolarization. In the presence of high external [K^+], however, the actual k_{off} value at hyperpolarized voltages is much greater than that predicted from the unblock measurements made at more depolarized voltages, suggesting that a mechanism exists to destabilize the toxin binding in the closed state (Fig. 4; also see below).

The effects of CTX and κ-conotoxin PVIIA have been analyzed in detail (Garcia et al., 1999; Terlau et al., 1999). The blocking mechanisms of these toxins with three disulfide bridges appear to be essentially similar to the mechanism of the maurotoxin action described here. Terlau et al. (1999) found the unblock phenomenon with depolarization, using PVIIA on ShBΔ6–46 channels expressed in oocytes. They also found that the dissociation rate constant k_{off} for the PVIIA action on the ShBΔ6–46 channel was much greater than that predicted by the unblock time course at depolarized voltages. Based on the results obtained by MacKinnon and Miller (1988) for CTX, they postulated that when the outermost K^+ binding site is occupied, binding of PVIIA is destabilized by repulsion, thus increasing the dissociation rate constant k_{off}. It is likely that a similar mechanism underlies the maurotoxin action. Our results, obtained with different internal [K^+] concentrations, indicate that the efflux of K^+ ions may repel the toxin molecule away from the channel and contribute to the voltage dependence of k_{off}, potentially affecting the outermost K^+ binding site. The difficulty associated with manipulating both the intracellular and extracellular solutions in the same experiment, however, makes it impractical to quantitatively assess how internal and external [K^+] may differentially affect the toxin efficacy.

Clearance of K^+ from the channel pore is considered to accelerate the C-type inactivation time course (López-Barneo et al., 1993), which is likely to involve constriction of the channel pore at the external segment (Liu et al., 1996). According to the model proposed by Terlau et al. (1999), K^+ in the Shaker channel destabilizes the toxin binding. Clearing the channel pore of K^+ during C-type inactivation may be expected to enhance the toxin binding, thus making the C-type inactivated state more sensitive to the toxin. Our results, however, show that the Na^+ flux through the C-type inactivated state is not appreciably affected by maurotoxin. Several possible interpretations of this finding exist. Na^+ may cause a very rapid dissociation of the toxin from the channel. The Na^+ flux may proceed unimpaired, even with the toxin bound to the channel. The conformational change from the open state to the C-type inactivated state, likely involving constriction of the pore (Liu et al., 1996), may directly destabilize the toxin binding. The observation that residue 449 in the external mouth of the pore regulates both C-type inactivation (López-Barneo et al., 1993) and the toxin efficacy (see Fig. 6) suggests that the toxin binding stability is dependent on the local protein conformations near residue 449. This is consistent with the last possibility that the toxin binding is destabilized by transition to the C-type inactivated state.

The work presented here shows that position 449 in the outer mouth of the channel has an important influence on the maurotoxin action. Position 449 on the Shaker channel is also involved in CTX binding, and it interacts with M29 in CTX (Naranjo and Miller, 1996). This residue is replaced in a conservative manner by an I at position 25 in maurotoxin, which may indicate that I25 could play a key role in mediating the toxin action on the Shaker channel. K23 in maurotoxin also appears to play a function similar to that of K27 in CTX for its interaction with Shaker channels, inasmuch as K23A mutation decreases the toxin affinity by 1000-fold (Carlier et al., 2000). These results suggest that the equivalent key residues in maurotoxin could mediate the Shaker pore recognition (see also discussion of Fig. 7 below). κ-Conotoxin PVIIA also interacts with the channel via the amino acid residues in the outer mouth of the pore, although the binding of CTX and PVIIA with the channel may involve different molecular interactions (Shon et al., 1998). Position 449 is in part involved in external TEA binding, C-type inactivation, and external K^+ sensitivity (Molina et al., 1997; López-Barneo et al., 1993). The ShBΔ6–46:T449V channel expressed in oocytes does not show noticeable C-type inactivation, and it is not markedly affected by external [K^+]. The toxin efficacy on this channel at −90 mV is less [K^+] dependent than that on the ShBΔ6–46 channel with faster C-type inactivation. It may be speculated that in the ShBΔ6–46:T449V channel the external K^+ binding site that is important in the toxin affinity is occupied by a K^+ ion more frequently, decreasing the toxin efficacy and interfering with C-type inactivation.

To infer how different amino acid residues of maurotoxin are involved in its interaction with the channel pore, we aligned the three-dimensional structures of maurotoxin and charybdotoxin obtained from Protein Data Bank. Fig. 7 *A* shows the aligned averaged structures of the two toxins. Distances between Cα's of the corresponding residues of the two toxins are shown in Fig. 7 *B*. This alignment shows that the Cα deviation distances were typically less than 2 Å. The triplet, K27:M29:N30, and the doublet, R34:Y36, in charybdotoxin are well conserved among different K^+

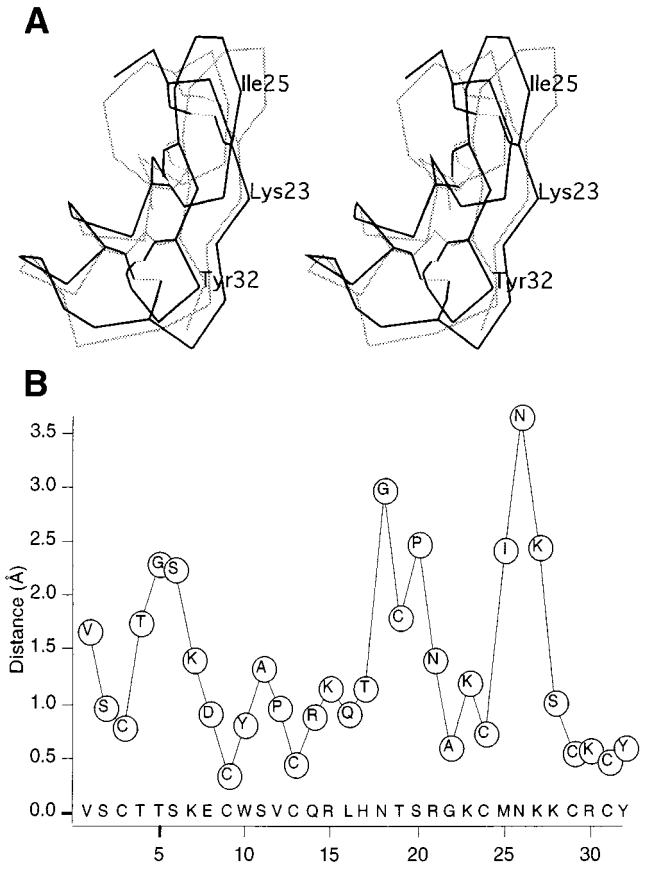

FIGURE 7 Structural alignment of charybdotoxin and maurotoxin. (*A*) Stereoscopic view of backbone Cα alignment of maurotoxin (*black lines*, PDB entry 1TXM) and charybdotoxin (*gray lines*, PDB entry 2CRD). Each structure shown represents the average of all structures contained in corresponding PDB files. Side chains of cysteine residues are also shown to display disulfide bridges (shown with *thin lines*). Alignment was performed with an iterative fit method, as implemented in SwissPDBViewer. (*B*) Distances between Cα atoms in corresponding residues of two toxins for alignment shown in *A*. Residues of maurotoxin are shown inside data points; corresponding residues for charybdotoxin are shown along the horizontal axis. The horizontal axis shows residue numbering in maurotoxin.

channel toxins, and they play critical roles in the interaction of the toxin with the channel (Goldstein et al., 1994; Savarin et al., 1999). Among those residues K27 is known to protrude into the pore and interacts with potassium ions in the pore (Goldstein and Miller, 1993). M29 interacts with T449 of the Shaker channel (Naranjo and Miller, 1996), and Y36 also interacts with T449 in a different subunit (Dauplais et al., 1997). These residues correspond to K23:I25:N26 and K30:Y32 in maurotoxin. Although the alignment indicates that I25:N26 in maurotoxin shows a considerable divergence from the corresponding M29:N30 in charybdotoxin, the relative positions of these residues within the K:I:N triplet structure are essentially the same in the two toxins (7.0 Å K to M/I, 3.8 Å M/I to N, 10.2/10.5 Å N to K in charybdotoxin/maurotoxin). The turn of the β-sheet containing the triplet is packed more closely with the rest of the toxin in maurotoxin than in charybdotoxin, accounting for the large deviation around position 26 (Fig. 7 *B*). The structural alignment reveals that the two toxins share similar structural motifs; however, the relative contributions of the key amino acid residues to the toxin-channel interaction in maurotoxin could be different from those in CTX because of the differential disulfide bridge patterns. Mutant cycle experiments to determine the relative importance of the residues in the triplet and doublet would be of particular interest.

We thank A. Freet and Dr. J. Thommandru for technical assistance, Dr. E. Shibata for helpful comments on the manuscript, and Eddie Jones for amplifier settings.

This work was supported in part by American Heart Association grant 9601440.

REFERENCES

Anderson, C. S., R. MacKinnon, C. Smith, and C. Miller. 1988. Charybdotoxin block of single Ca^{2+}-activated K^+ channels. Effects of channel gating, voltage, and ionic strength. *J. Gen. Physiol.* 91:317–333.

Carlier, E., V. Avdonin, S. Geib, Z. Fajloun, R. Kharrat, H. Rochat, J.-M. Sabatier, T. Hoshi, and M. E. De Waard. 2000. Effect of maurotoxin, a four disulfide-bridged toxin from the chactoid scorpion *Scorpio maurus*, on *Shaker* K^+ channels. *J. Pept Res.* 55:419–427.

Catterall, W. A., and D. A. Beneski. 1980. Interaction of polypeptide neurotoxins with a receptor site associated with voltage-sensitive sodium channels. *J. Supramol. Struct.* 14:295–303.

Chung, S. H., and P. W. Gage. 1998. Signal processing techniques for channel current analysis based on hidden Markov models. *Methods Enzymol.* 293:420–437.

Dauplais, M., A. Lecoq, J. Song, J. Cotton, N. Jamin, B. Gilquin, C. Roumestand, C. Vita, C. L. C. de Medeiros, E. G. Rowan, A. L. Harvey, and A. Menez. 1997. On the convergent evolution of animal toxins. Conservation of a diad of functional residues in potassium channel-blocking toxins with unrelated structures. *J. Biol. Chem.* 272: 4302–4309.

Garcia, E., M. Scanlon, and D. Naranjo. 1999. A marine snail neurotoxin shares with scorpion toxins a convergent mechanism of blockade on the pore of voltage-gated K channels. *J. Gen. Physiol.* 114:141–157.

Goldstein, S. A., and C. Miller. 1993. Mechanism of charybdotoxin block of a voltage-gated K^+ channel. *Biophys. J.* 65:1613–1619.

Goldstein, S. A., D. J. Pheasant, and C. Miller. 1994. The charybdotoxin receptor of a Shaker K^+ channel: peptide and channel residues mediating molecular recognition. *Neuron.* 12:1377–1388.

Hamill, O. P., A. Marty, E. Neher, B. Sakmann, and F. J. Sigworth. 1981. Improved patch-clamp techniques for high-resolution current recording from cells and cell-free membrane patches. *Pflugers Arch.* 391:85–100.

Hermann, A., and C. Erxleben. 1987. Charybdotoxin selectively blocks small Ca-activated K channels in *Aplysia* neurons. *J. Gen. Physiol.* 90:27–47.

Hoshi, T., W. N. Zagotta, and R. W. Aldrich. 1990. Biophysical and molecular mechanisms of *Shaker* potassium channel inactivation. *Science.* 250:533–538.

Hoshi, T., W. N. Zagotta, and R. W. Aldrich. 1991. Two types of inactivation in *Shaker* K^+ channels: effects of alterations in the carboxy-terminal region. *Neuron.* 7:547–556.

Hoshi, T., W. N. Zagotta, and R. W. Aldrich. 1994. *Shaker* potassium channel gating. I. Transitions near the open state. *J. Gen. Physiol.* 103:249–278.

Kharrat, R., K. Mabrouk, M. Crest, H. Darbon, R. Oughideni, M. F. Martin-Eauclaire, G. Jacquet, M. el Ayeb, J. Van Rietschoten, H. Rochat, and J. M. Sabatier. 1996. Chemical synthesis and characterization of maurotoxin, a short scorpion toxin with four disulfide bridges that acts on K^+ channels. *Eur J Biochem.* 242:491–498.

Kharrat, R., P. Mansuelle, F. Sampieri, M. Crest, R. Oughideni, J. Van Rietschoten, M. F. Martin-Eauclaire, H. Rochat, and M. El Ayeb. 1997. Maurotoxin, a four disulfide bridge toxin from *Scorpio maurus* venom: purification, structure and action on potassium channels. *FEBS Lett.* 406:284–290.

Lebrun, B., R. Romi-Lebrun, M. F. Martin-Eauclaire, A. Yasuda, M. Ishiguro, Y. Oyama, O. Pongs, and T. Nakajima. 1997. A four-disulphide-bridged toxin, with high affinity towards voltage-gated K^+ channels, isolated from *Heterometrus spinnifer* (Scorpionidae) venom. *Biochem. J.* 328:321–327.

Liu, Y., M. E. Jurman, and G. Yellen. 1996. Dynamic rearrangement of the outer mouth of a K^+ channel during gating. *Neuron.* 16:859–867.

López-Barneo, J., T. Hoshi, S. H. Heinemann, and R. W. Aldrich. 1993. Effects of external cations and mutations in the pore region on C-type inactivation of *Shaker* potassium channels. *Receptors Channels.* 1:61–71.

MacKinnon, R., and C. Miller. 1988. Mechanism of charybdotoxin block of the high-conductance, Ca^{2+}-activated K^+ channel. *J. Gen. Physiol.* 91:335–349.

Methfessel, C., V. Witzemann, T. Takahashi, M. Mishina, S. Numa, and B. Sakmann. 1986. Patch clamp measurements on *Xenopus laevis* oocytes: currents through endogenous channels and implanted acetylcholine receptor and sodium channels. *Pflugers Arch.* 407:577–588.

Miller, C. 1995. The charybdotoxin family of K^+ channel-blocking peptides. *Neuron.* 15:5–10.

Molina, A., A. G. Castellano, and J. Lopez-Barneo. 1997. Pore mutations in Shaker K^+ channels distinguish between the sites of tetraethylammonium blockade and C-type inactivation. *J. Physiol. (Lond.).* 499: 361–367.

Naranjo, D., and C. Miller. 1996. A strongly interacting pair of residues on the contact surface of charybdotoxin and a Shaker K^+ channel. *Neuron.* 16:123–130.

Olamendi-Portugal, T., F. Gomez-Lagunas, G. B. Gurrola, and L. D. Possani. 1996. A novel structural class of K^+-channel blocking toxin from the scorpion *Pandinus imperator*. *Biochem. J.* 315:977–981.

Park, C. S., and C. Miller. 1992. Interaction of charybdotoxin with permeant ions inside the pore of a K^+ channel. *Neuron.* 9:307–313.

Rochat, H., R. Kharrat, J. M. Sabatier, P. Mansuelle, M. Crest, M. F. Martin-Eauclaire, F. Sampieri, R. Oughideni, K. Mabrouk, G. Jacquet, J. Van Rietschoten, and M. El Ayeb. 1998. Maurotoxin, a four disulfide bridges scorpion toxin acting on K^+ channels. *Toxicon.* 36:1609–1611.

Savarin, P., R. Romi-Lebrun, S. Zinn-Justin, B. Lebrun, T. Nakajima, B. Gilquin, and A. Menez. 1999. Structural and functional consequences of the presence of a fourth disulfide bridge in the scorpion short toxins: solution structure of the potassium channel inhibitor HsTX1. *Protein Sci.* 8:2672–2685.

Selisko, B., C. Garcia, B. Becerril, F. Gomez-Lagunas, C. Garay, and L. D. Possani. 1998. Cobatoxins 1 and 2 from *Centruroides noxius* Hoffmann constitute a subfamily of potassium-channel-blocking scorpion toxins. *Eur. J. Biochem.* 254:468–479.

Shon, K. J., M. Stocker, H. Terlau, W. Stuhmer, R. Jacobsen, C. Walker, M. Grilley, M. Watkins, D. R. Hillyard, W. R. Gray, and B. M. Olivera. 1998. kappa-Conotoxin PVIIA is a peptide inhibiting the Shaker K^+ channel. *J. Biol. Chem.* 273:33–38.

Starkus, J. G., L. Kuschel, M. D. Rayner, and S. H. Heinemann. 1997. Ion conduction through C-type inactivated Shaker channels. *J. Gen. Physiol.* 110:539–550.

Terlau, H., A. Boccaccio, B. M. Olivera, and F. Conti. 1999. The block of Shaker K^+ channels by kappa-conotoxin PVIIA is state dependent. *J. Gen. Physiol.* 114:125–140.